REDUCING CONCENTRATIONS OF INELASTIC DEMAND WITH A STRONGBACK

Barbara G. Simpson[1]

ABSTRACT

Multi-story braced frames exhibit large variations in inelastic demand over the building height and tend to concentrate damage in a few weak stories during an earthquake. This paper presents the numerical and experimental results of a "strongback" system, a modification of the conventional braced frame that utilizes a vertical steel truss to delay or prevent weak-story behavior. A cyclic test was performed on a nearly full-scale two-story strongback retrofit design. The design was composed of two halves: an "inelastic" truss utilizing a buckling-restrained brace (BRB) to dissipate energy and an "elastic" truss designed to engage both stories to mitigate weak-story behavior. The strongback specimen was effective in impeding the formation of a weak-story mechanism and in mobilizing the reserve strength of other structural components, even after rupture of the BRB core. Test results established that the strongback can be a viable method of mitigating weak-story behavior. A calibrated numerical model was able to predict the global response of the frame, including the rupture of the BRB using a low-cycle fatigue material model. Satisfactory agreement was obtained in comparisons of experimental and numerical results.

INTRODUCTION

A number of numerical studies have indicated that conventional braced frames tend to concentrate damage in a few "weak" stories during strong earthquakes (Khatib *et al*. 1988, Tremblay 2003, Chen and Mahin 2010, Lai and Mahin 2015). These studies have been corroborated through experimental tests (Foutch *et al.* 1987, Simpson *et al*. in press) and post-earthquake observations (Rai and Goel 2003) showing similar behavior. After buckling, the strength of a brace tends to degrade upon subsequent loading cycles. Thus, brace buckling in a story causes that story to become relatively weaker than the stories that have remained elastic. This relative reduction in story strength and stiffness promotes larger demands in stories with earlier or larger inelastic deformations. In multi-story braced frames, the braces may be unable to re-distribute this demand to other stories in the system, eliciting weak-story behavior; Fig. 1(a). These concentrations of demand can trigger greater localized structural and nonstructural damage, exacerbate residual drifts, and make repairs impracticable or uneconomical.

Many researchers have explored various methods of reducing concentrations of damage in braced frames. Several approaches include: [i] providing a "back-up" system that utilizes framing action to carry the loss of local story shear capacity upon brace bucking, as in a dual system (Foutch *et al.* 1987, Whittaker *et al.* 1990); [ii] the use of slender braces with relatively large tension-to-compression capacities to better re-distribute the forces from the compression brace to the tension brace (Tremblay 2003, Chen and Mahin 2010); [iii] the use of buckling-restrained braces (BRBs) with relatively large strain hardening capable of engaging adjacent stories upon yielding (Tremblay 2003); [iv] detailing the columns in both the lateral and gravity systems to help carry the load upon brace buckling, as in the continuous column or similar gravity-supplemented concepts (MacRae *et al.* 2004,

[1] Ph.D. Candidate, Dept. of Civil and Environmental Eng., University of California, Berkeley, CA

Ji *et al*. 2009); and [v] adopting alternative bracing configurations better suited to distribute inelastic demands over the building height; as in the zipper frame (Khatib *et al*. 1988).

However, while dual systems have been recognized in building codes for several decades, it is unclear how strong and stiff the backup frame should be to achieve a desired performance goal (Khatib *et al*. 1988) and the surrounding frame must be increased to resist the moments induced by frame action (Tremblay 2003). The braces used in approach [ii] and [iii] may result in large beam sizes and substantial overstrength; impacting the size of the columns, foundations, and surrounding structural elements. The distributed nature of the continuous column raises a number of design issues related to seismic detailing of the gravity load system and could potentially complicate the distribution of lateral forces to the columns in the gravity load system. Finally, subsequent research of the zipper frame found it difficult to find the appropriate member sizes needed to achieve a desired response (Yang *et al.* 2009).

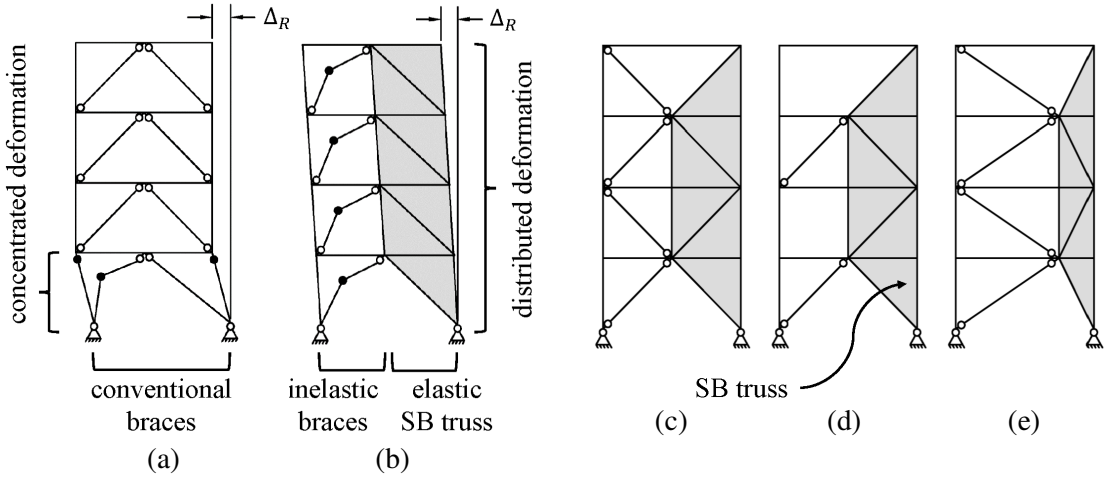

FIGURE 1. (a) Conventional braced frame; (b) SB system; (c-e) alternative SB brace configurations.

The "strongback" (SB) method examined in this study is a hybrid of the zipper frame (Khatib *et al*. 1988), tied eccentric braced frame (Popov *et al*. 1992), and elastic truss system (Tremblay 2003, Mar 2010) that utilizes a vertical steel "backbone" to mitigate weak-story behavior. The SB system is a relatively simple and economic modification of the conventional braced frame that utilizes two vertical trusses; Fig. 1(b). The "inelastic" truss is detailed to dissipate energy through either conventional brace buckling and yielding behavior or buckling-restrained braces (BRBs). The opposite "elastic" truss, or strongback, is intended to distribute story drifts and inelastic demands; thereby delaying or preventing a weak-story. The strongback is pinned at its base and designed to remain essentially elastic, forcing adjacent stories to undergo similar lateral deformations during an earthquake. In this manner, the strongback is able to impose a nearly uniform response over the building height. Other possible SB configurations are shown in Fig. 1(c-e). Alternatively, the SB truss could be represented be a concrete or steel plate shear wall (Qu *et al.* 2012, Djojo *et al.* 2014).

The strongback mobilizes energy dissipation in the entire system, averages damage across multiple stories, and reduces peak inelastic demands; thereby increasing safety, reducing damage, and minimizing red or yellow tagging following a major earthquake. The strongback also provides a reliable means of redistributing internal forces. For instance, braces can be removed, e.g. by failure or for architectural reasons, provided the strongback is strong enough to bridge across multiple stories; Fig. 1(d). While the strongback may require extra strength to remain elastic, this cost could be balanced by use of ordinary details in the elastic truss, the utilization of the same brace cross section and connection details at every story, and a reduction of the strength or number of braced frames if a reduced redundancy factor could be justified (Panian *et al.* 2015).

Research to date on "masted" systems like the SB system has focused primarily on applications to new construction. Moreover, few experimental studies have examined the efficacy of such systems, as past research has focused on computational simulation of the seismic response (Tremblay 2003, Lai and Mahin 2015, Panian *et al.* 2015). Thus, the experimental and numerical study described herein was undertaken to establish whether the strongback is a viable method of mitigating weak-story behavior. A strongback retrofit strategy was implemented to prevent the weak-story response observed during two previous experiments on "vintage" braced frames. This paper briefly summarizes the experimental results of these two previous tests. The remainder of this paper outlines the experimental design, test setup, and test results for a two-story, one bay strongback retrofit scheme. The nearly full-scale test specimen utilized a BRB in the "inelastic" truss and hollow (HSS) braces in the "elastic" truss. Test results from the strongback are then compared to simulations using nonlinear numerical analyses.

TEST SPECIMENS

Three planar specimens of two older concentric braced frames (CBFs) and one strongback retrofit were tested at Berkeley as part of the study reported herein. This paper focuses on the third test specimen, designated NCBF-B-3SB, which consisted of an SB retrofit of the first two test specimens, designated NCBF-B-1 and NCBF-B-2. All three test specimens were two-stories tall by one-bay wide.

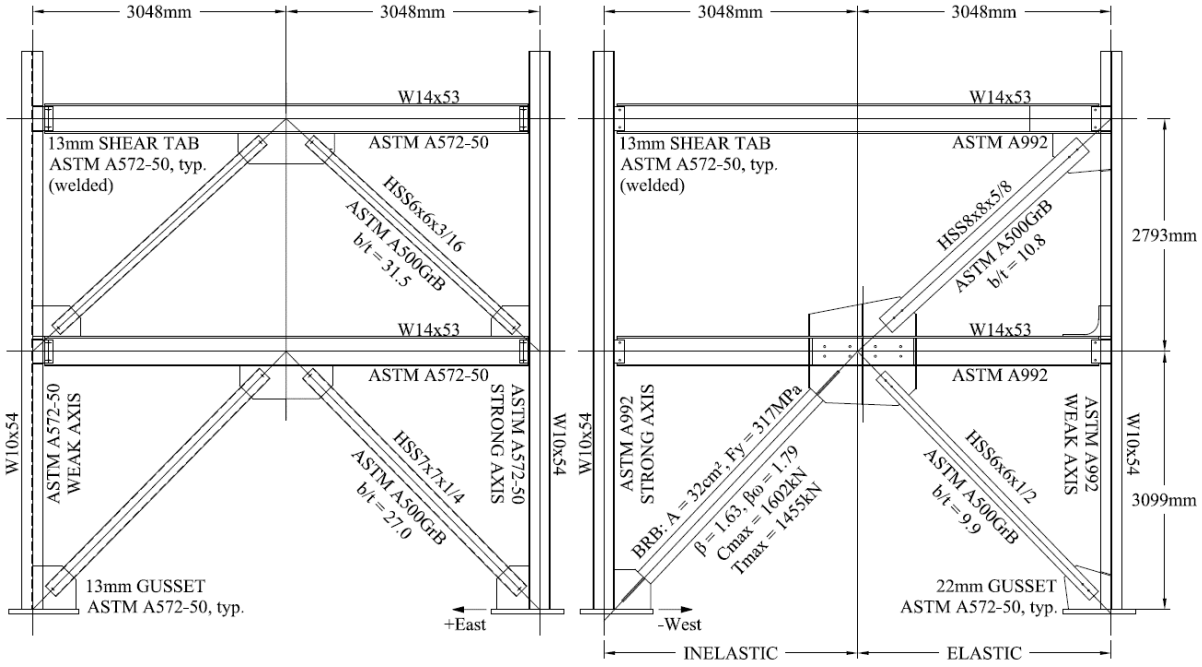

(a) (b)

FIGURE 2. Test specimen schematic: (a) older braced frame tests; (b) SB retrofit test.

Vintage Braced Frame Tests

Both vintage braced frame specimens had similar connection details, member sizes, and material specifications; Fig. 2(a). The original two test specimens utilized square HSS braces placed in a "chevron" configuration with one column oriented in strong-axis bending and the other in weak-axis bending. The first specimen (NCBF-B-1) was typical of vintage construction in 1985 (ICBO 1985) and did not satisfy current seismic design requirements. This specimen exhibited severe brace local buckling and premature brace fracture before forming a weak second story; Fig. 3(a).

The second upgraded specimen (NCBF-B-2) utilized braces filled with low-strength concrete

to delay the local buckling observed during the first test. The second specimen exhibited a weak first story with one fractured brace, causing the first floor beam to provide a weak and flexible secondary energy dissipating mechanism; Fig. 3(b). Relevant observations included: [i] fracture at the strong-axis column-to-baseplate interface due to the nearly rigid body motion of the plastic mechanism in Fig. 3(b); [ii] punching failures at the weak-axis unstiffened column web; and [iii] severe local buckling in the first floor beam plastic hinge region. Test results from both specimens illustrated that older braced frames are highly susceptible to weak-story behavior and local failure mechanisms. The third strongback specimen aimed to address observations [i-iii] and the recurring weak stories; see Fig. 3(c).

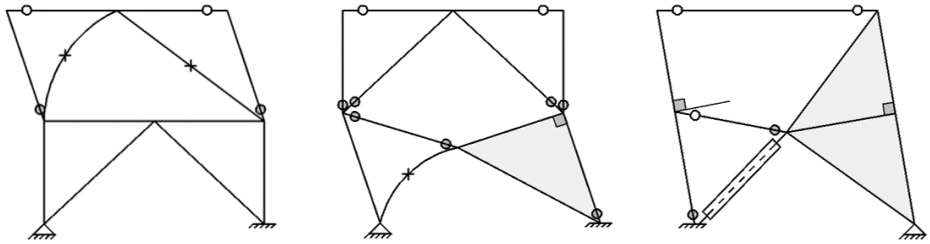

(a) (b) (c)

FIGURE 3. Plastic mechanism: (a) NCBF-B-1, (b) NCBF-B-2, and (c) NCBF-B-3SB

Strongback Design

The third test specimen (NCBF-B-3SB) implemented a “strongback” retrofit scheme to address the weak-story tendency observed during the first two tests; Fig. 3(c). The retrofit design was based on the original design of the two previous tests. To minimize the need for demolition and shoring in an actual retrofit situation the beams, columns, and shear tabs from the original design were retained for the SB retrofit. The original "chevron" braces were replaced with new braces and gusset plates in a re-oriented “strongback” geometry. The new lambda configuration, Fig. 2(b), consisted of two trusses:

1. The column, braces, and half beam on the west (right) side of the frame in Fig. 2 were designed to remain essentially elastic throughout the test. The west column and braces were intended to act like a strong backbone (or “strongback”) for the system.

2. The lateral load resisting system on the east (left) side of the frame consisted of a single buckling restrained brace (BRB) that acted as the primary energy-dissipating device in the system. Other plastic deformations were expected at the ends of the east first floor half beam, the base of the east column, and the east shear tab connections at the lower and roof beams.

Member sizes were reverse engineered considering the specimen geometry, a lateral load applied at the first floor equal to half that applied at the second floor and the maximum base shear capacity of the test setup (approximately 2,670kN (600kips)). Based on the maximum test setup base shear, a BRB was selected to have a core area of 32cm^2 (5in^2). A BRB with welded end details was selected based on relatively large erection tolerances considered suitable for retrofit situations.

The remaining braces in the elastic strongback were chosen based the maximum forces that could be delivered to the surrounding system from the BRB. This assumed the plastic mechanism shown in Fig. 4(a). The elastic braces were designed to be 1.1 times these forces at incipient collapse, as shown by the moment and axial force diagrams in Fig. 4(b,c). In these diagrams, positive moments are counterclockwise and positive axial forces are tensile. Because they were expected to remain elastic, net section reinforcement and compact sections were not used for the elastic brace sections.

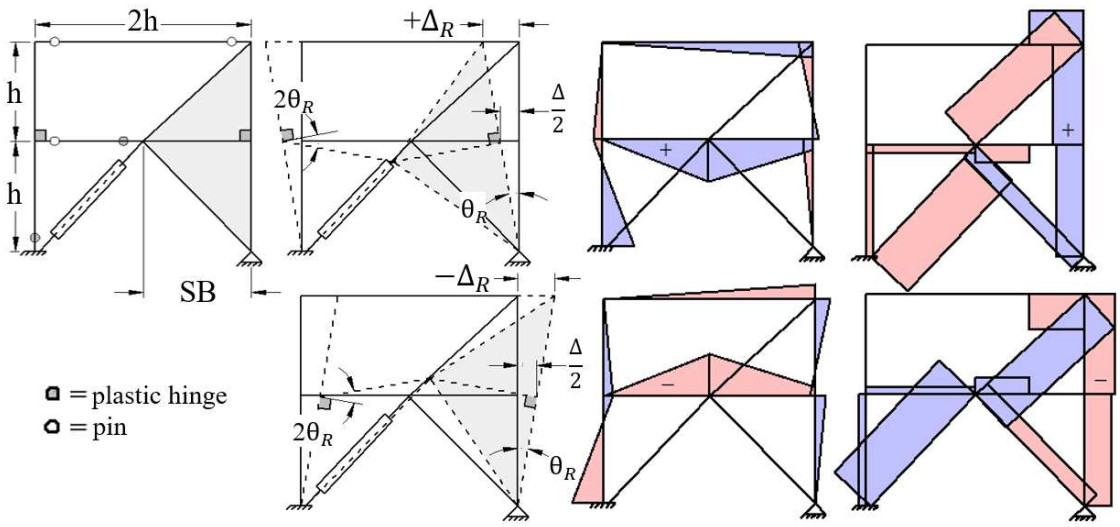

FIGURE 4. Idealized SB system: (a) kinematic, (b) moment, and (c) axial force diagrams

The beam and column sections were kept the same as the original NCBF-B-1 design. A plastic hinge was expected to develop near the center connection of the first floor beam after the BRB had yielded; Fig. 4(a). Though the BRB was designed as the primary energy dissipating mechanism, the beam was expected to secondarily dissipate energy through yielding of this plastic hinge region. As such, the original beam size was design checked as a long shear link in an eccentrically braced frame. The beam's shear strength was considered to be critical, so the web of the original beam was reinforced with doubler plates at the center and roof west gusset connection.

Large plastic rotations were also anticipated at the base of the west column in the strongback, Fig. 3(a). Hence, the column in the strongback was oriented in weak-axis bending to mimic a "pinned" connection. This secondarily addressed the large rotation demand (Fig. 3(b)) and subsequent failure of the column-to-baseplate interface observed during the NCBF-B-2 test. The weak-axis column was additionally reinforced with stiffeners at the column web near the connection regions to address local web punching failures observed during the NCBF-B-2 test.

New gusset connections were designed for the ends of all bracing members based on current seismic provisions (AISC 2010) and capacity design principles. Stiffeners were used on either side of this middle gusset to force the expected beam plastic hinging outside of the center connection, based on severe beam local buckling observed in the NCBF-B-2 test. All welded shear tabs were initially kept the same as the NCBF-B-1 design. Shear tabs were welded, rather than bolted, to the beams and columns to be consistent with the welds used for the gusset-to-column interface originally located above those regions. Due to the difficulty in acquiring non-notch tough welding consumables, the welds at the shear tab locations were specified as notch-tough and were consistent with current design standards.

Test Setup

The test utilized an existing setup configuration from a previous study; Fig. 5(a). Two MTS 980kN (220kip) actuators (see "4") were located at each floor level. The two actuators were connected directly to the quarter-points of the beams through heavy transfer brackets (see "5") at each floor. Fixed conditions were provided at the column baseplates through CJP welds at the baseplate-to-column interface. Lateral out-of-plane support was provided by a stiff vertical support frame (see "6"). The columns were attached to the test setup through steel plates that acted like transverse shear tabs (see

"8"), allowing beam elongation and shortening through yielding of the plates. A center support (see "9") running vertically along the frame centerline was also attached to the test setup in the same fashion. This center support is only connected to the test setup and does not touch the experimental specimen. The center support provided out-of-plane lateral stability at the midpoint of the beams while also providing a safety measure against expected large vertical beam displacements.

The loading protocol was based on the horizontal displacement of the roof beam. The roof actuators were displacement-controlled and the first floor actuators were force-controlled. The forces in the lower level actuators were set to be half the force feedback from the load cells in the roof actuators. This arrangement maintained an inverted triangular load distribution over the height of the frame with a maximum base shear of approximately 2670MPa (600kips). The tests followed a loading protocol similar to current cyclic qualification testing provisions for BRBs (AISC 2010) for a target design roof drift ratio of 2%; Fig. 5(b). Additional amplitude cycles were used to monitor the strongback behavior under deformations similar to that imposed for specimens NCBF-B-1 and NCBF-B-2 and to observe damage at larger roof displacements. A coat of whitewash was applied to the constructed specimen to aid in identifying areas of high strain; Fig. 5(c).

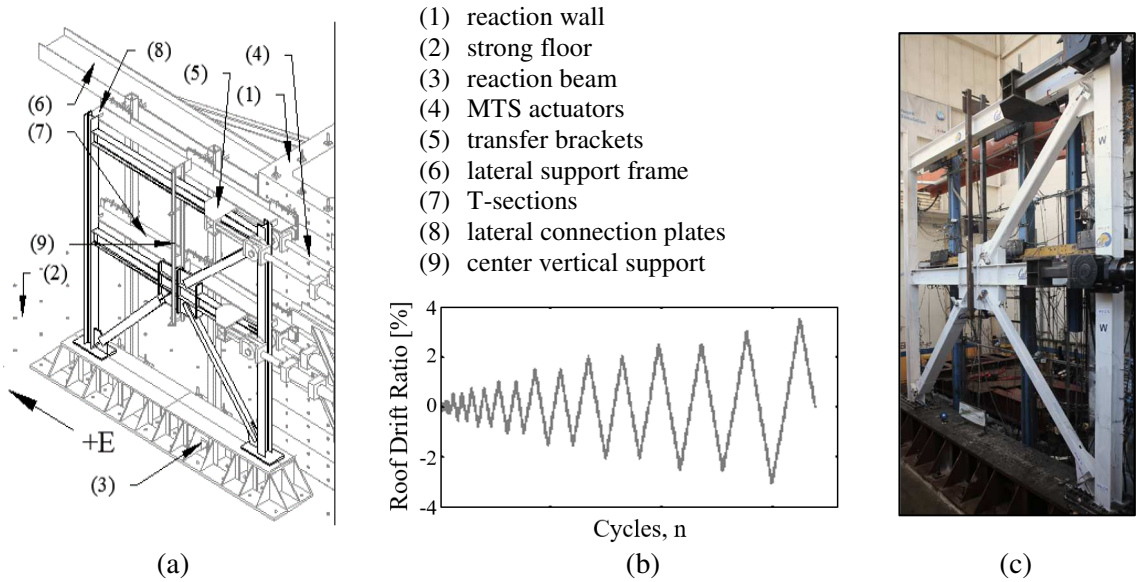

FIGURE 5. (a) Test setup, (b) Loading protocol, (c) Constructed test specimen.

TABLE 1. Major observations.

Event Point	Location	Damage description	Amplitude (%)	Cycle no.	θ_R (%)	θ_1 (%)	θ_2 (%)
1	1st floor BRB	yielding	+0.5	1	+0.21	+0.18	+0.25
2	1st floor east shear tab (#1)	fracture	-1.5	1	-1.43	-1.38	-1.49
3	1st floor BRB	fracture	+2.5	1	+1.45	+1.37	+1.56
4	2nd floor east shar tab (#1)	fracture	+2.5	1	+2.49	+2.42	+2.56
5	Test end	residual drift			+0.61	+0.58	+0.65

EXPERIMENTAL OBSERVATIONS

Displacements are considered positive when the frame moves in the east (left) direction of the laboratory and negative when the frame moves in the west (right) direction, as shown in Fig. 5(a). The

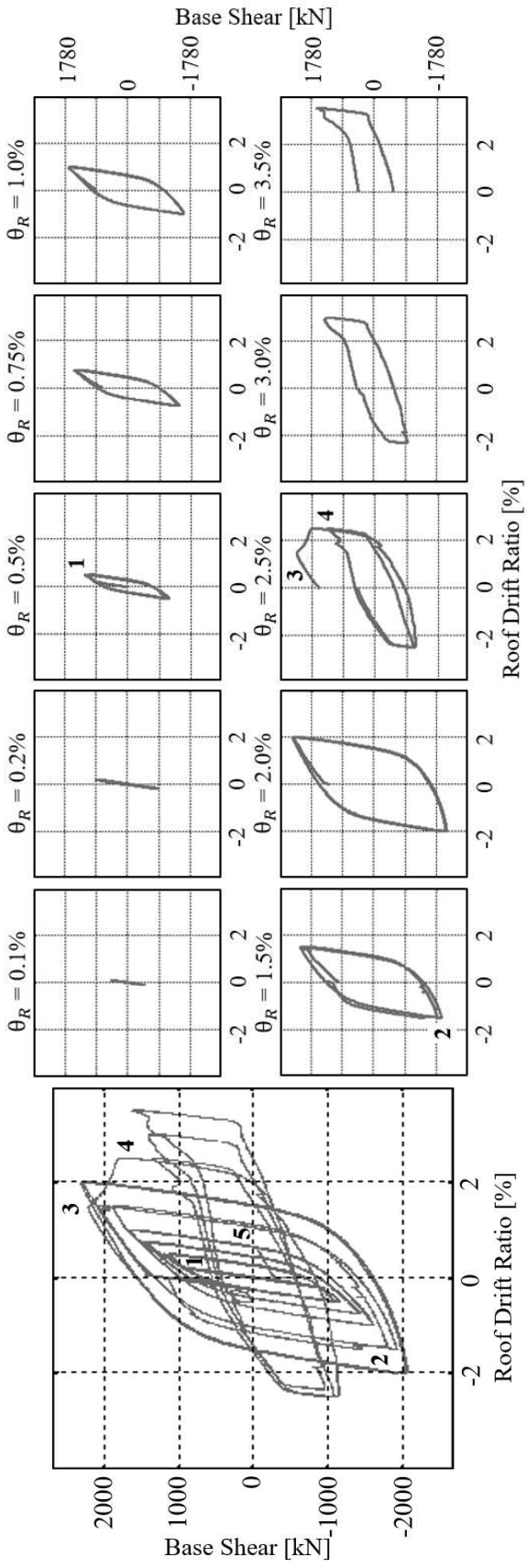

FIGURE 6. Global hysteresis.

roof drift ratio, θ_R, is defined as the lateral displacement of the top-level actuators divided by the total frame height. First- and second-story drift ratios, θ_1 and θ_2, are defined as the lateral displacement of the floor minus the displacement of the floor below divided by its respective story height. Fig. 6 shows the global hysteresis shape and a breakdown of the hysteretic loops by cyclic amplitude. Observations numbered in the figures are described in Table 1.

The SB system performed as intended, maintaining nearly uniform lateral drift over both stories over the complete loading protocol. The specimen went through the entire displacement history, including two complete cycles at the target amplitude, θ_R = 2%, without observed deterioration of its hysteretic behavior. The hysteretic loops through the 2% roof drift cycles were full and stable and looked like that of a typical BRB frame. During the first quarter cycle to θ_R = 2.5%, the outer casing of the BRB bulged, Fig. 7(a), and the frame exhibited a softening response; θ_R = 2.5% in Fig. 6. However, the strongback was able to continue to avoid a weak-story for the remainder of the test. While the stiffness and strength of the frame was reduced, the frame was still able to dissipate energy through smaller, but stable, hysteretic loops produced by the stiffness and strength of the remaining members; $\theta_R \geq$ 2.5% in Fig. 6. Residual drifts at the end of the test in both the first and second stories were similar; Table1.

Both braces in the strongback remained essentially elastic. The BRB exhibited kinematic and isotropic strain hardening after yielding at θ_R = 0.5% in Fig. 6. A large drop in the load-carrying capacity of the BRB was observed during θ_R = +2.5% when the BRB was in compression. It is assumed that the brace subsequently ruptured in tension during that same cycle to θ_R = –2.5%, as it appeared to contribute little tensile capacity in later cycles. The BRB did contribute some capacity in compression after rupture when the sections of the fractured core came in contact with one another; θ_R = 3.5% in Fig. 6. Despite relatively high axial strains, the BRB satisfied current cyclic testing requirements for BRBs (AISC

2010) until the target amplitude of θ_R = 2.0%. The BRB was able to develop a normalized cumulative plastic deformation of 421 before the system showed a significant loss in strength and stiffness

Plastic hinges formed where expected, as predicted by the kinematic diagram of Fig. 4(a). A plastic hinge developed in the first floor beam just to the east of the middle gusset connection; Fig. 7(b). The beam exhibited secondary energy dissipation through plastic yielding and web and flange local buckling after rupture of the BRB. The first floor beam was induced to move up and down significantly because of the strongback's induced rigid body rotation, see Fig. 4(a). The strongback effectively linked the vertical displacement of the center of the beam to the lateral displacement of the roof, causing the beam to move a maximum of 70mm (2.76") upward and 96mm (3.78") downward. Plastic hinges also developed at the base of both the east and west columns. These regions performed well during the test and showed no signs of crack initiation or fracture. The east, strong-axis column had small axial loads throughout the test, and most of its yielding was isolated to the external east column flange. The weak-axis column was able to go through large rotational demands, acting much like a "pin" base.

(a) (b) (c) (d) (e)

FIGURE 7. Observed damage: (e) BRB, (f) center gusset, (a) first floor east shear tab (#1), (b) first floor east shear tab (#2), (c) second floor east shear tab (#1)

The majority of the connection regions behaved well during the test. The punching failures observed during the older braced frame tests appear to have been mitigated by the addition of stiffeners at the weak-axis column web. Whitewash flaking at the gusset plates indicated minor yielding. Small amounts of whitewash flaking was also observed at the net section region of the elastic braces. The first floor middle connection had very little observable yielding at the end of the test; see Fig. 7(b). Other than the welded shear tab connections, the connections were considered to be "new" retrofitted details designed according to capacity design principles and behaved well and as expected.

Rotations at the first floor beam-column region were approximately double the applied roof drift ratio; Fig. 4(a). The welded shear tab (#1) details at the east column on the first floor and roof level were both inadequate for the rotational demands induced in these regions. The shear tab-to-beam weld failed at the east first floor connection at θ_R = 1.5%, corresponding to an in-plane rotational demand of 0.03 radians; Fig. 7(c). The shear tab was replaced by a shear tab with slotted holes (#3) to prevent large moment demands from developing at this region; see Fig. 7(d). The new connection behaved well, and experienced only minor yielding between the bolt holes of the shear tab connection. During θ_R = 2.5%, the shop shear tab-to-column weld failed at the east roof connection; see Fig. 7(e). This shear tab was not previously damaged and was presumed adequate since it had only half of the rotational demands of the first floor shear tab; see Fig. 4(a). After failure, the beam was allowed to cantilever off the west column for the remainder of the test.

TEST COMPARISON

Table 2 includes a summary of the three specimens tested in this program. The older braced

frame tests yielded at a roof drift ratio more than double that of the SB test specimen. The first two test specimens were, therefore, able to remain elastic at much higher drift demands than the third SB retrofit scheme. However, inelastic behavior, while delayed in the first two tests, also initialized a dramatic loss in stiffness and strength due to brace buckling in the first two test specimens. The backbone curve in Fig. 8(a) shows that strength degradation occurred very quickly after brace buckling in the first two NCBF-B-1 and 2 test specimens. On the other hand, the BRB in the NCBF-B-3SB test specimen showed steady strain hardening after yielding until BRB rupture.

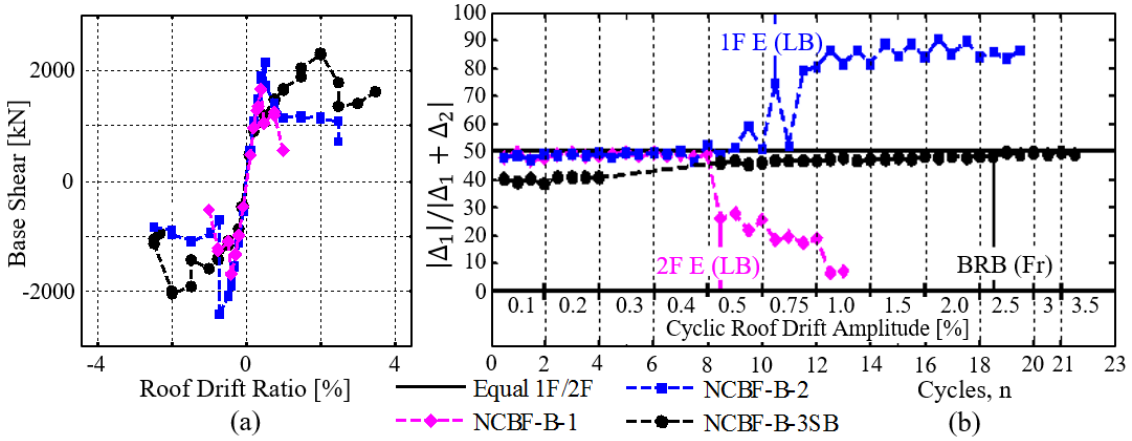

FIGURE 8. Test comparison: (a) hysteretic envelope; (b) weak-story tendency.

TABLE 2. Summary of test results.

specimen name:	NCBF-B-1	NCBF-B-2	NCBF-B-3SB
description:	Baseline pre-'88 CBF	CFT upgrade	SB retrofit
maximum base shear:	1722kN (387kips)	2412kN (542kips)	2323kN (522kips)
roof drift ratio at yield[a]:	0.41%	0.51%	0.21%
maximum roof drift ratio[b]:	0.44%	0.77%	2.0%
weak-story location:	second story	first story	no weak-story

[a] Yield = first signs of significant global nonlinear behavior triggered by buckling or yielding.
[b] Maximum roof drift ratio prior to significant strength degradation defined when the measured base shear dropped below 80% of the specimen's maximum capacity.

In all three cases, fracture of a brace was associated with a drop in strength and stiffness. Fracture resulted a dramatic loss of strength to roughly 30% of the frame's original capacity in NCBF-B-1 and 2. In the case of the second test, NCBF-B-2, this loss in strength was slowly recovered upon repeated cycles as the beam began to act as a secondary energy-dissipation mechanism; Fig. 3(b). However, this recovery was limited by other damage states, i.e., connection failures in other parts of the system. In the case of the SB retrofit scheme, loss in strength after BRB rupture was not as severe. The beam was able to provide some secondary back-up resistance, and the strongback continued to engage the energy dissipation of the remaining frame.

The tendency for each test to form a weak-story is plotted in Fig. 8(b). This tendency is defined by the ratio of the first story drift, Δ_1, to the total drift, $\Delta_1 + \Delta_2$. The second and first story for the NCBF-B-1 and 2 tests, respectively, contributed disproportionately more to the total after the start of their strength deterioration, indicative of weak stories; Fig. 3(a,b). In both cases, local buckling, defined by the label (LB), in a story corresponded to the largest jump in that story's drift contribution. In contrast, the SB retrofit scheme exhibited similar drift ratios in both stories throughout the entire test; Fig. 3(c).

The first-story drifts in the SB frame varied little from the solid line at the 50% ratio in the plot, indicating nearly equal story drift levels in the first and second stories. This plot illustrates the ability of the SB system to sustain a uniform drift distribution even after BRB rupture (Fr).

NUMERICAL PREDICTION

An analytical phase implemented in the structural analysis framework, OpenSEES (McKenna 1997), was used to predict the response of the experimental test. The elastic braces were modelled with two force-based nonlinear beam-column elements with initial imperfections and corotational transformations to allow them to buckle out-of-plane; Fig. 9(a). The BRB was modelled as one element and utilized a low-cycle fatigue material model (Uriz and Mahin 2008) to capture rupture. Fiber sections were used to model the cross-sectional shape of the elements and rigid end zones were used for the beam-column connections and gusset plates. Possible connection failures at the beam-column and gusset regions were not modeled. Information on the numerical parameters can be found in Table 3.

TABLE 3. Numerical input parameters.

Level	Modeling parameter	BRB	braces	beams, columns
Element	Number of elements	1	2	1
	Number of integration points	5	5	5
Section	Number of fibers along B	10	4	4
	Number of fibers along t_f	-	4	4
	Number of fibers along t_w	4	4	2
Steel material (menegotto-Pinto)	Strain hardening, b	0.03	0.03	0.03
Fatigue materal	ε_0	0.10	-	-
	m	-0.458	-	-

B = section width; t_f = flange thickness; t_w web thickness; ε_0 and m = empirical fatigue parameters.

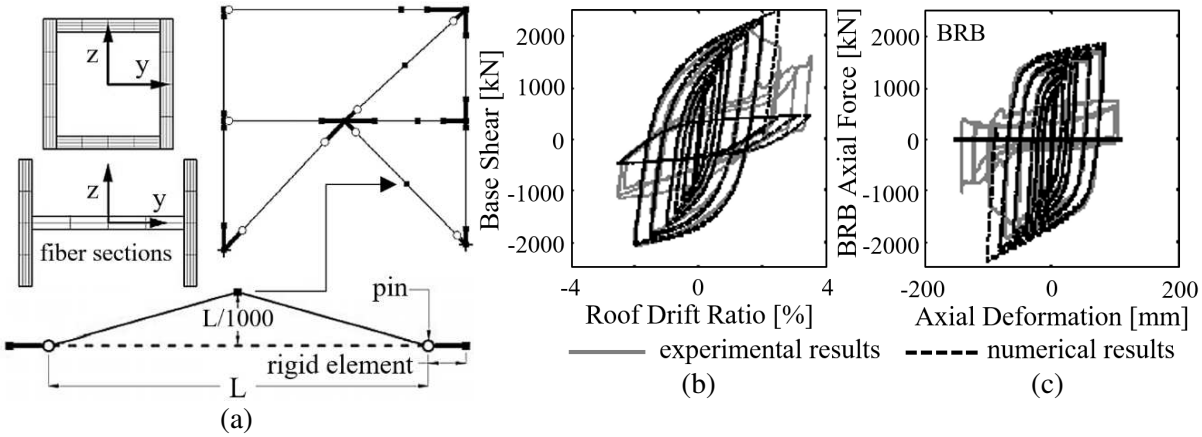

FIGURE 9. Numerical prediction: (a) model schematic; (b) global response; (c) BRB response.

Plots of the global and BRB hysteretic shapes from the experimental test and numerical model are overlaid for comparison purposes in Fig. 9(b) and (c). It is clear that the overall behavior is mostly predicted by the simulation models, including BRB rupture. The low-cycle fatigue model, however, only allows the BRB to rupture in tension, thus the softening response is a half cycle delayed in the simulation as the BRB ruptured in compression during the test; see Fig. 9(c). After BRB rupture, the BRB contributes no stiffness or strength to the numerical model. In the case of the experiment, some reserve capacity was observed in the steel core as the two fractured ends came in contact in compression

and pulled apart in tension. This reserve capacity from this contact is not simulated, as shown by the differences in later hysteretic cycles after BRB rupture.

SUMMARY AND CONCLUSIONS

This experimental and numerical study examined a "strongback" retrofit strategy aimed at mitigating the weak-story behavior observed during two previous experiments. The strongback utilized a vertical steel truss that was designed to remain essentially elastic; thereby engaging both stories to prevent concentrations of damage. The "strongback" retrofit was successful in mitigating weak-story behavior and work is currently underway to develop and refine design methods for the strongback using the results of this experimental test and ongoing numerical analyses. To summarize –

1. The SB system behaved well and as intended, mitigating a weak-story mechanism even after rupture of the BRB, the primary energy-dissipating mechanism. The BRB satisfied current cyclic testing protocols before rupture, and the beam was capable of participating as a secondary energy-dissipation mechanism through plastic hinging near the middle gusset connection. The weak-axis column was also capable of large rotational demands, allowing the "strongback" half of the system to reach relatively large lateral displacements. The components of the "elastic" truss exhibited only minor damage at the end of the loading protocol, and plastic hinge regions were well predicted by a simple kinematic diagram of the frame's plastic mechanism; Fig. 4. Residual drifts indicate that re-centering capabilities may be required to ensure the frame's viability after an earthquake. Further optimization of the elastic half of the system could provide smaller, yet adequate, brace sections.

2. The geometry of the lambda configuration induces strains in the BRB and rotational demands in some beam-column connections that are about double that of a conventional braced frame that disallows vertical translation of the beam; Fig. 4(a). An offset geometry, like that of Fig. 1(e), would allow for longer yield lengths in the BRBs and smaller beam-column rotations; thereby reducing instances of damage at these locations. Furthermore, while the use of a slotted shear tab connection reduced both the rotation and moment demands at the beam-column connections, the slotted shear tab also allows for net elongation and shortening between the end of the beam and the column flange. Future designs at this location may need to consider this residual movement and either restrain this movement or provide supplemental re-centering.

3. A calibrated numerical model was able to capture the experimental results with considerable accuracy. The use of fiber-based elements to model hysteretic behavior and the use of an empirical low-cycle fatigue material to capture BRB rupture were key to the model's effectiveness. However, these fiber elements do not directly account for the effects of local buckling and they must be calibrated to experimental results to ensure their reliability. More detailed models considering connection failures may be required to capture behaviors not modeled for this numerical study.

ACKNOWLEDGEMENTS

This project would not have been possible without the substantial contributions of Schuff Steel and StarSeismic who donated the steel fabrication and the buckling-restrained brace. The author would like to extend a special thanks to Prof. Stephen Mahin, the co-PI and advisor for this project, whose advice and feedback was indispensable, and to the technical staff of the George E. Brown, Jr., Network for Earthquake Engineering Simulation (NEES) laboratory at Berkeley for their invaluable assistance during the test. This research was supported by National Science Foundation (NSF) under grant number CMMI-1208002. The findings, opinions, and recommendations or conclusions in this paper are those of the author alone and do not necessarily reflect those of the National Science Foundation.

REFERENCES

AISC (2010). "Seismic provisions for structural steel buildings." *ANSI/AISC-341-10*, American Institute of Steel Construction, Chicago.

Chen, C.H., Mahin, S.A. (2012). "Performance-based seismic demand assessment of concentrically braced steel frame buildings." *Rept. PEER-2012/103*, Pacific Earthquake Engineering Research Center, Univ. of California, Berkeley, CA.

Djojo, G.S., Clifton, G.C., Henry, R.S. (2014). "Rocking steel shear walls with energy dissipation devices." *Proc., New Zealand Society for Earthq. Eng. Conference*, Aukland, New Zealand.

Foutch, D. A., Goel, S. C., Roeder, C. W. (1987). "Seismic testing of full-scale steel building—Part I." J. Struct. Eng., 10.1061/(ASCE)0733-9445(1987)113:11(2111), 2111–2129.

ICBO (1985). *Uniform building code*, International Conference of Building Officials, Whittier, CA.

Ji, X., Kato, M., Wang, T., Hitaka, T., Nakashima, M. (2009). "Effect of gravity columns on mitigation of drift concentration for braced frames." *J. Constr.Steel Research*, *65*(12), 2148–2156.

Khatib, I.F., Mahin, S.A., Pister, K.S. (1988). "Seismic behavior of concentrically braced frames." *Rept. UCB/EERC-88/01*, Earthquake Engineering Research Center, Univ. of California, Berkeley, CA.

Lai, J. and Mahin, S. (2014). "Strongback System: A Way to Reduce Damage Concentration in Steel-Braced Frames." *J. Struct. Eng.*, 10.1061/(ASCE)ST.1943-541X.0001198, 04014223.

MacRae, G., Kimura, Y., Roeder, C. (2004). "Effect of Column Stiffness on Braced Frame Seismic Behavior." *J. Struct. Eng.*, 10.1061/(ASCE)0733-9445(2004)130:3(381), 381-391.

Mar, D., (2010). "Design examples using mode shaping spines for frame and wall buildings." *Proc., 9th U.S. National and 10th Canadian Conf. on Earthquake Engineering*, Earthquake Engineering Research Institute, Oakland, CA.

McKenna, F. (1997). "Object Oriented Finite Element Programming Frameworks for Analysis, Algorithms and Parallel Computing." *Ph.D. Dissertation*, Department of Civil and Environmental Engineering, University of California, Berkeley, CA.

Panian, L., Bucci, N., Janhunen, B. (2015) BRBM Frames: An Improved Approach to Seismic-Resistant Design Using Buckling-Restrained Braces. Improving the Seismic Performance of Existing Buildings and Other Structures 2015: pp. 632-643. doi: 10.1061/9780784479728.052

Popov, E.P., Ricles, J.M., Kasai, K. (1992). "Methodology for optimum EBF link design." *Proc., 10th World Conf. on Earthquake Engineering*, CRC Press/Balkema, Rotterdam, Netherlands.

Qu, Z., Wada, A., Motoyui, S., Sakata, H., Kishiki, S. (2012). Pin-supported walls for enhancing the seismic performance of building structures. *Earthquake Engineering & Structural Dynamics* vol. 41 (14) p. 2075-2091

Rai, D.C., Goel, S.C. (2003). "Seismic evaluation and upgrading of chevron braced frames." *J. Constr. Steel Res.*, *59*(8), 971–994. http://doi.org/10.1016/S0143-974X(03)00006-3

Simpson, B.G., Mahin, S.A., Lai, J.W. (in press). "Cyclic Testing of Older Steel Braced Frames." *Rept. No. PEER-2017/XX*, Pacific Earthquake Engineering Research Center, Berkeley, CA.

Tremblay, R. (2003). "Achieving a stable inelastic seismic response for multi-story concentrically braced steel frames." *AISC Eng. J.*, 40(2), 111–129.

Whittaker, A.S., Uang, C.M., Bertero, V. (1990). "An experimental study of the behavior of dual steel systems." *Rept. UCB-EERC-88/14*, Earthquake Engineering Research Center, Univ. of California, Berkeley, CA.

Uriz, P., Mahin, S. A. (2008). "Toward earthquake resistant design of concentrically braced steel-frame structures." *Rept. PEER-2008/08*, Pacific Earthquake Engineering Research Center, University of California, Berkeley, CA.

Yang, C. S., Leon, R. T., and DesRoches, R., (2009). "Performance Evaluation of Innovative Steel Braced Frames." PEER Rep. 2009/103, Pacific Earthquake Engineering Research Center, Univ. of California, Berkeley, CA.